



HAL
open science

Phase Equilibrium Studies of High-Pressure Natural Gas Mixtures with Toluene for LNG Applications

Saif Zs. Al Ghafri, Thomas J.R. Hughes, Fernando Perez, Corey J Baker, Arman Siahvashi, Armand Karimi, Arash Arami-Niya, Eric F May

► **To cite this version:**

Saif Zs. Al Ghafri, Thomas J.R. Hughes, Fernando Perez, Corey J Baker, Arman Siahvashi, et al.. Phase Equilibrium Studies of High-Pressure Natural Gas Mixtures with Toluene for LNG Applications. Fluid Phase Equilibria, 2020, 518, pp.112620. 10.1016/j.fluid.2020.112620 . hal-02875150

HAL Id: hal-02875150

<https://ifp.hal.science/hal-02875150>

Submitted on 19 Jun 2020

HAL is a multi-disciplinary open access archive for the deposit and dissemination of scientific research documents, whether they are published or not. The documents may come from teaching and research institutions in France or abroad, or from public or private research centers.

L'archive ouverte pluridisciplinaire **HAL**, est destinée au dépôt et à la diffusion de documents scientifiques de niveau recherche, publiés ou non, émanant des établissements d'enseignement et de recherche français ou étrangers, des laboratoires publics ou privés.

Phase Equilibrium Studies of High-Pressure Natural Gas Mixtures with Toluene for LNG Applications

Saif ZS. Al Ghafri^a, Fernando Perez^a, Arman Siahvashi^a, Corey J. Baker^a, Armand Karimi^a, Thomas J. Hughes^{a,b}, Arash Arami-Niya^a and Eric F. May^{a*}

^a *Fluid Science and Resources Division, Department of Chemical Engineering, University of Western Australia, Crawley, WA 6009, Australia*

^b *Resources Engineering Program, Department of Civil Engineering, Monash University, Clayton, Victoria 3800, Australia*

*Corresponding Author: eric.may@uwa.edu.au

ABSTRACT

To prevent possible freeze out in the main cryogenic heat exchanger (MCHE) used in liquefied natural gas (LNG) plants, new and accurate phase equilibrium data are required to improve the predictive reliability of existing models, in particular cubic equations of state (EOS). In this work, the vapor-liquid equilibrium (VLE) of a ternary methane + propane + toluene (methylbenzene) mixture was studied over a wide range of conditions with toluene as the minor component in both the liquid and vapor phases. Measurements were conducted along different isochoric paths at temperatures between (213 and 298 K) and pressures up to 8.3 MPa, to obtain data at conditions relevant to the operation of LNG scrub columns. The measured VLE data were compared to results calculated with the HYSYS Peng Robinson (PR) equation of state (EOS) that is used widely in LNG industry. The amount of toluene in the vapour phase was found to be under-predicted by the HYSYS PR EOS by an average of around 77 % at lower temperatures, with the error increasing as temperature and toluene concentration decreased. The current work demonstrates that the HYSYS PR EOS as well as other cubic EOS substantially under-predict the possible toluene content of saturated vapours that could be present in the overhead of the LNG scrub column. Using the ThermoFAST model recently developed and optimised for the calculation of solid-liquid equilibrium conditions in LNG production, this work further demonstrates that the 77% increase in the toluene content of a saturated vapour entering the MCHE, corresponds to a 7 K increase in the solid formation temperature, which could significantly increase the likelihood of a blockage in the MCHE and thus possible shutdown of the LNG plant. The experimental and modelling work presented here underscores the importance of improving predictions of the allowable threshold concentration of heavy components in fluids entering cryogenic heat exchangers in LNG plants.

Key words: VLE, methane, propane, toluene, natural gas, LNG, scrub column, Peng Robinson, freeze out

1. Introduction

Liquefied Natural Gas (LNG) plants are known to be energy and cost-intensive, requiring a large amount of power for the processes of treatment, compression and refrigeration, and with special designed equipment such as the main cryogenic heat exchangers (MCHE), refrigerant compressors and cryogenic distillation towers. [1] Before natural gas is liquefied, impurities such as acid gases, water and heavy hydrocarbons must be removed [2]. Treated natural gas then enters a cryogenic distillation tower known in the industry as a 'scrub column' (SC) to remove the heavy hydrocarbons [1]. The lean gas stream then enters the main cryogenic heat exchanger (MCHE) where the liquefaction occurs.

An illustrative schematic for a typical scrub column schematic is shown in Figure 1. The scrub column operates essentially at a constant pressure, the value of which depends upon the feed pressure and composition. Typically, the scrub column conditions are around 4-6 MPa with its feed gas pre-cooled and partially condensed at a temperature that depends on its composition [3]. The treated gas is cooled in the MCHE to about $-151\text{ }^{\circ}\text{C}$ (122 K) producing a high pressure LNG, which then enters a turbine or a flash expansion valve to provide further cooling to about $-160\text{ }^{\circ}\text{C}$ (113 K) at (or near) atmospheric pressure. Several natural gas liquefaction technologies have been proposed for the production of LNG [4-9] but each stage of that transformation process is designed using predictions of the mixture's thermophysical properties as a function of temperature, pressure and composition. A detailed and accurate simulation is thus essential for the design, operation and optimization of the LNG liquefaction and treatment processes, which is influenced substantially by the accuracy of the property model used in the simulation [10, 11].

The scrub column's purpose [3] is to prevent significant concentrations of compounds heavier than propane (C_{3+}) from entering the MCHE, so that (a) the LNG meets its heating value specification and (b) compounds heavier than pentane (C_{5+}) do not freeze-out and block the narrow tubing networks within the MCHE which can lead to severe consequences including unplanned plant shutdowns. The hydrocarbons in natural gas that pose the greatest risk of forming solids are the so called BTEX (benzene, toluene, ethylbenzene and xylenes) compounds. Benzene, for example, has a normal melting temperature of $5.45\text{ }^{\circ}\text{C}$ [12], and a solubility of only around 5 ppm in LNG at ($-150\text{ }^{\circ}\text{C}$, 5 MPa) [13].

In the scrub column, separation of the heavy components from the natural gas destined for the MCHE is achieved by maintaining a temperature gradient along the SC vertical length and by ensuring intimate contact between the liquid and vapor phases either in trays and/or packing distributed along the column's length. These trays or a length of the packing are considered as stages in which the sequence of VLE-based separations occurs. In an ideal system, the vapor and liquid phases would reach equilibrium at each "theoretical stage", with the vapor then moving up the column to a colder tray and the liquid moving down to a warmer tray. The vapor is therefore flashed sequentially at decreasing temperatures allowing the heavier hydrocarbons to be stripped out and condensed. The condensed liquid flows down the column and is flashed sequentially at increasing temperatures, liberating any light hydrocarbons that may be dissolved in it. This liquid stream produced from the bottom of the scrub column is usually processed further to extract additional sales products (LPG, condensates) and/or make-up refrigerant (C_2 , C_3^+) for use in the MCHE.

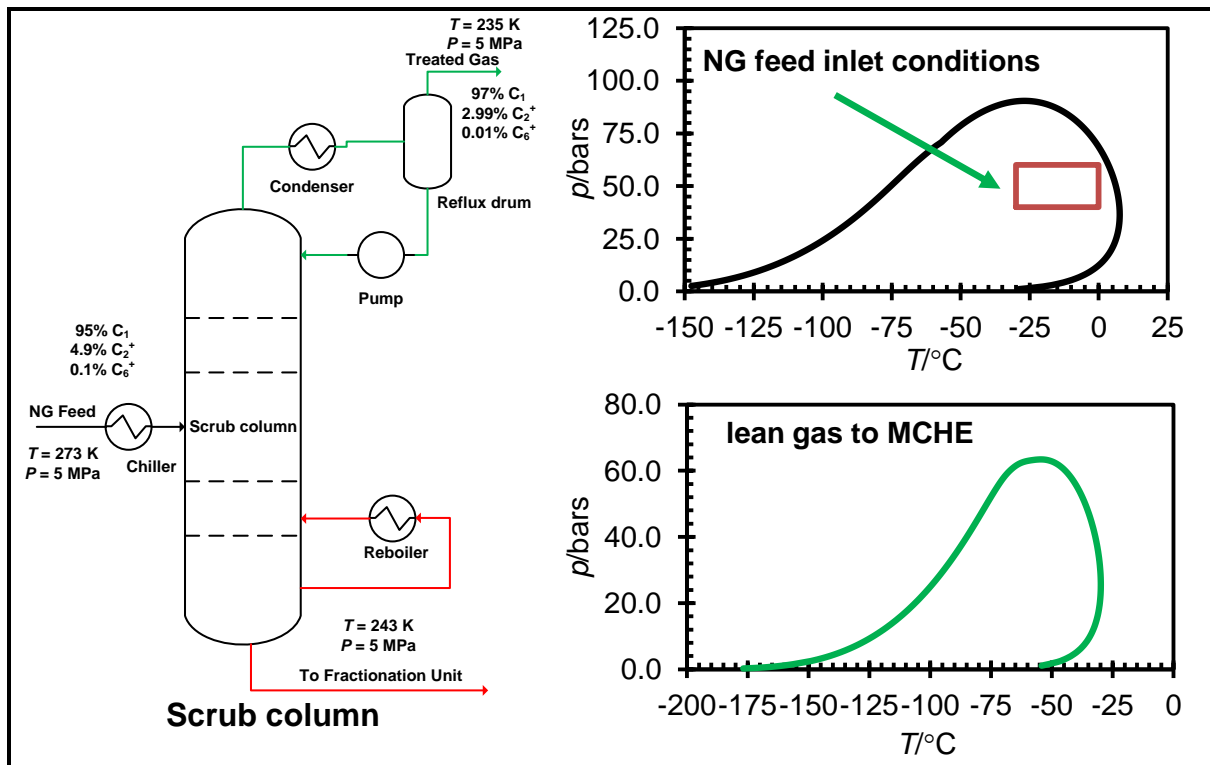


Figure 1. An Illustrative schematic of a cryogenic distillation column located prior to the main cryogenic heat exchanger in a liquefaction plant. Phase envelopes calculated using the GERG 2008 EOS [14] are shown both for synthetic mixture considered in this work as a feed to the column ($0.950C_1+0.049C_3+0.001\text{tol}$), and a vapour overheads outlet ($0.9700C_1+0.0299C_3+0.0001\text{tol}$) stream.

Simulation of the scrub column requires the simultaneous solution of three sets of equations representing the energy balance, material balance and phase equilibrium at each theoretical stage. The solution to these equations for the entire column is achieved iteratively using, for example, the inside/out convergence algorithm discussed by Russell [15]. Central to any solution algorithm is the reliable and efficient calculation of the thermodynamic properties of each mixture on each tray: this includes the distribution at equilibrium of the components between the two phases (the $K_i = y_i / x_i$ values), the phase enthalpies, and the phase volumes. The most important of these are the K_i values and the phase enthalpies.

However, the uncertainty associated with the thermodynamic models used by the simulator to calculate these quantities has a direct impact on the reliability of the simulation and therefore, the required operating margins employed. Several authors have examined the impact of thermodynamic uncertainties on the reliability of process simulations [16, 17]. Kister [18] has reviewed several examples of problems associated with the simulation of distillation columns and identified the inability to predict K_i values as the leading cause of problematic simulations. Thus, the selection of the most appropriate thermodynamic model for use in the process simulation of the scrub column is critical. Determining the most appropriate model requires an assessment of the performance of possible equations of state (EOS) against data obtained in laboratory experiments and / or from operating LNG plants. The latter, however, are difficult to obtain and often have comparatively large uncertainties that make it difficult to distinguish between the EOS used in the process simulations [19].

Most recent efforts to improve LNG process simulations have focussed on the use of complex equations of state capable of more accurately describing the vapour-liquid equilibrium and heat capacities of multi-component fluid mixtures [10, 11, 14, 20, 21]. However, the industry still uses cubic equations of state (EOS) such as PR76 [22] developed by Peng and Robinson, and RKS [23] developed by Redlich, Kwong and Soave. There are many types of EOS with varying complexity but all are anchored to measured data and the EOS reliability decreases as predictions go beyond the data range. For example, whilst the reference GERG-2008 EOS by Kunz and Wagner [14] is recommended by NIST for natural gas mixtures, a highly complex multi-parameter equation requiring iterative solution, its VLE predictions are no more accurate than those of the cubic EOS used by process simulators because of their computational efficiency. Dauber and Span [10] examined the influence of different models on the simulation of the LNG liquefaction process and LNG transport. They have concluded that GERG-2008 EOS provides the highest potential for accurate calculations of the thermodynamic properties of natural gas such as density, heat capacity and enthalpy. However, in their work, the composition of the LNG considered was representative of the feed entering the MCHE and didn't include heavy hydrocarbons (C_{6+}).

To determine which EOS is best for the description of heavy hydrocarbon carry-over in LNG scrub columns requires accurate experimental data. However, such data are scarce, particularly for the multi-component mixtures and high-pressure conditions of most relevance to industrial LNG columns. In 2015, May et al. [20] reported reference-quality p, T, x, y measurements describing the VLE of binary mixture for methane + ethane, + propane, + 2-methylpropane (isobutane), and + butane that clearly identified deficiencies in EOS commonly used by industry, and in several of the archival literature data to which those models have been tuned. We have also studied the VLE of methane + toluene binary mixtures at temperatures from (179 to 313) K [24] as well as methane + pentane, and methane + hexane binary mixtures at temperatures from (173 to 330) K [25]. However, while these results can be used to tune equations of state, they do not provide stringent tests of the phase compositions found in an LNG plant where a range of intermediate compounds is also present. Accordingly, in this work we investigated the VLE of the methane + propane + toluene system with the objective of investigating conditions where toluene is a minor component in *both* the liquid and vapour phases. Measurements of the VLE of this ternary mixture were conducted at temperatures between 213 and 298 K and pressures up to 8.3 MPa.

The measured VLE data for this ternary system were compared to results calculated with the AspenTech HYSYS Peng Robinson (PR) equation of state (EOS) [26]. While both phases were measured and all the data obtained are reported here, the focus of the comparisons was on the ability of the EOS to correctly predict the toluene content of the vapor phase, as this relates directly to the risk of cryogenic solids formation in the MCHE and the operational performance of the scrub column.

2. Experimental Section

2.1 Materials

The suppliers and supplier-analysed purities of all components used in this work are listed in Table 1. No further purification was applied.

Table 1. Source and purities of chemicals used in this work

Compound	Supplier	Purity	CAS
Methane	BOC	0.99999	74-82-8
Propane	BOC	0.99995	74-98-6
Toluene	Sigma Aldrich	0.998	108-88-3
Heptane	Sigma Aldrich	0.99	142-82-5

2.2 Experimental Setup

Two apparatus were used for the VLE measurements, and the consistency of their results further increased the confidence in the results obtained. The first apparatus was described in detail previously [20, 25, 27-29] and referred to hereafter as the 'Cryostat VLE cell'. Only a summary is given here for completeness. The apparatus (Figure 2) comprised of an equilibrium cell with an inner volume of 60 ml and a maximum working pressure of up to 30 MPa. The cell was located inside a cryogenic Dewar (CRY) equipped with an automatic liquid nitrogen pump (LNP) that filled and controlled the liquid nitrogen level inside the Dewar. The temperature of the sample fluid was controlled by means of using a foil-type heating element that was wrapped and glued to the outer surface of the cell using high thermal conductivity epoxy suitable for cryogenic operation.

A motor was used to generate a rotating magnetic field, which in turn drove a Teflon-coated magnetic bar sitting inside the cell on the bottom surface to mix the sample fluid. Two 100 Ω PRTs mounted on the top and the bottom of the equilibrium cell were used for temperature measurements. These two PRTs were calibrated to ITS-90 by their supplier (LakeShore Cryotronics) over the temperature range of these experiments. The PRTs were also calibrated against a reference SPRT (ASL-WIKA) with a standard uncertainty of 0.02 K. The overall standard uncertainty of the cell temperature was estimated to be 0.2 K, taking into account temperature fluctuations. A pressure transducer (P1) (Kulite model CT-190), suitable for operation at temperatures from (77 to 393) K, was calibrated in situ by comparison with a reference quartz-crystal pressure transducer (Paroscientific Digiquartz series 1000) with a full scale of 14 MPa and a relative uncertainty of 0.008 % of full scale as stated by the manufacturer. The relative standard uncertainty of the Kulite transducer's calibration was 0.05 % for the pressure range from (1 to 14) MPa. Two capillary tubes with internal diameters of less than 0.015 cm were also mounted in the cell lid. One of the capillaries was used to sample the vapor phase in the cell while the other capillary was used to sample the liquid phase. One end of each capillary sampling tube was mounted inside a specialized Rapid On-Line Sampler Injector (ROLSI) electromagnetic solenoid valve for sampling analysis.

One key modification relative to our previous work was the use of a new gas chromatograph equipped with a capillary column (Agilent, PoraBOND Q, 25m, 0.53mm ID) and a barrier ionization discharge (BID) detector for the sample analysis. Such detectors are a relatively new technology developed by Shimadzu but are highly sensitive and can detect trace amounts of compounds. [30] This detector is 100 times more sensitive than a thermal conductivity detector (TCD) and two times more sensitive than a flame ionisation detector (FID), making it ideal for detecting the trace amounts of toluene in the vapor phase samples.

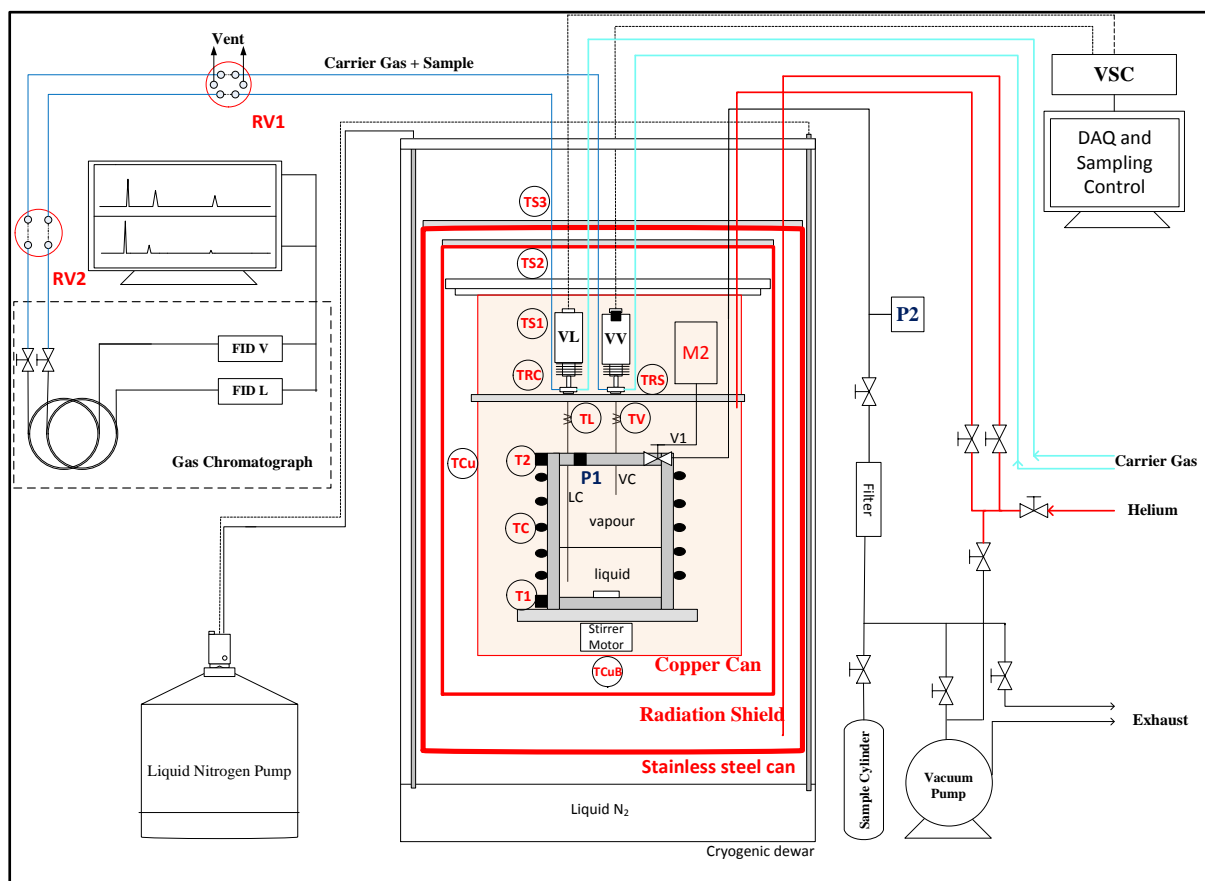


Figure 2. Schematic of the specialized cryogenic VLE apparatus (adopted from Ref. [27-29]).

The second apparatus (referred to hereafter as the 'Bath VLE cell'), comprised of an equilibrium cell with internal volume of 60 ml, maximum operating pressure of 30 MPa and with a liquid and vapor sampling valves identical to the first cell except that it was placed inside a temperature controlled liquid bath (LAUDA Alpha) rather than in a multi-can Dewar. The temperature of the system was controlled using a bath filled with a mixture of 0.5 ethylene glycol by weight in water. Two PRT sensors (NR-141-100S, Nitsushin) mounted on the top and bottom of the cell were used to measure temperature. The PRT sensors were calibrated by comparison with a standard platinum resistance thermometer (ASL-WIKA) in a constant temperature bath at temperatures up to 433 K. The standard uncertainty of the PRT was 0.05 K, but fluctuations of the bath temperature could be as much as ± 0.15 K. Consequently the overall standard uncertainty of the cell temperature was estimated to be 0.20 K. The system pressure was recorded using a quartz-crystal pressure transducer (Digiquartz, Parascientific) with a full scale of 13.8 MPa and a relative uncertainty of 0.01% of full scale connected to the top part of the equilibrium cell.

A variable speed motor was connected to a rotating gear attached to the bottom of the cell and generates a rotating magnetic field which in turn drives a PTFE coated magnetic bar sitting inside the cell on the bottom. This stirrer motor was used to mix the vapour and liquid phases until equilibrium was achieved. The composition of the liquid and vapour phase samples acquired from the Bath VLE cell was analyzed by a gas chromatograph (GC) equipped with a capillary column (Agilent, GS-GASPRO, 60m, 0.320mm ID) and a flame ionization detector (FID). This was achieved by using two capillary tubes with an internal diameter of less than 0.015 cm which were coupled with ROLSI electromagnetic solenoid valve to sample the liquid and vapor phases. The FID was sufficient because the Bath-VLE cell operated at higher temperatures, and thus the toluene concentration of the vapour phase samples was significantly higher than in the "Cryostat VLE cell". In both apparatus, the transfer tubes connecting the sampling valves to the respective GC were heated by means of low-voltage mineral-insulated heater cables operating with K-type thermocouple temperature sensors.

2.3 Experimental Procedure

To load each of the 60 ml cells, they were initially cleaned, flushed and evacuated and a small volume of about (1 to 3) ml of degassed toluene was injected into the equilibrium cell. The ternary mixture was then prepared either by pressurizing the cell with a gravimetrically-prepared, single-phase binary mixture of methane + propane (Bath VLE cell), or by cooling the apparatus to 273 K and condensing in propane in short bursts (Cryostat VLE cell). The stirrer in the cell was then turned on and methane was added in several bursts to get the pressure to the desired level. The system was then left for at least few hours to equilibrate while keeping the stirrer on to prompt mixing. Once the system was equilibrated, the gas and liquid phases were sampled by means of using the ROLSI valves. For each phase, at least 6 samples were taken and the results were continuously examined to ensure reproducibility. The sampling capillaries were flushed at least 10 times before samples were acquired and analyzed on the GC. Small amounts of liquid and gas sample were sent to the GC to avoid saturation of the GC column or its detector, and prevent any disturbance in the phase equilibrium and pressure inside the cell. Measurements were all made along isochoric pathways where the equilibrium cell was cooled into the two-phase region until a new desired temperature was reached.

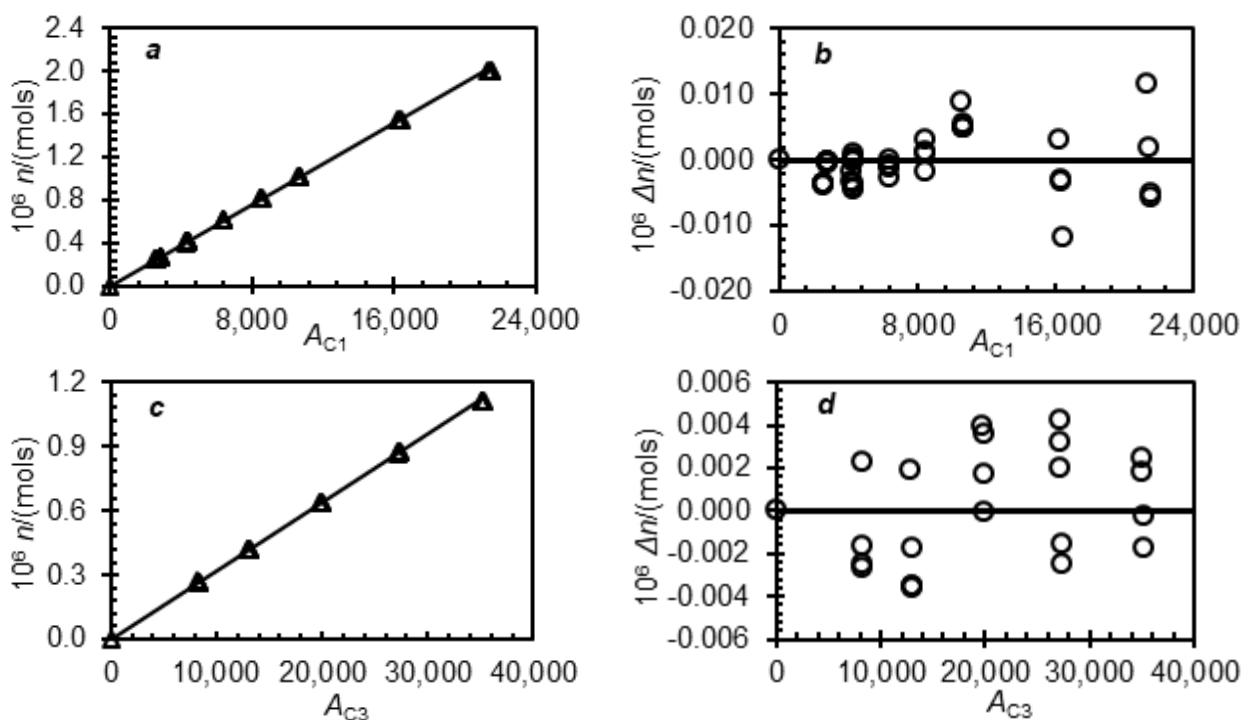
2.4 GC Calibration

A detailed description of the GC calibration procedures using either a relative or an absolute methods can be found in our previous work [20, 30-32]. Here the responses of the BID and FID detectors were calibrated for each component with an absolute method where the amount of substance injected into the GC is taken to be proportional to the density of the fluid at the sampling conditions.

The response of the FID or BID detectors to varying amounts of methane or propane was determined by adjusting the conditions of pressure and temperature in the sampling loops (Valco 0.2 and 0.5 μ L). The methane density was obtained from the EOS developed by Setzmann and Wagner [33] with an estimated relative uncertainty between 0.03% and

0.07%. The propane density was obtained from the EOS developed by Lemmon et al. [34] with an estimated relative uncertainty between 0.01% and 0.03% below 350 K. The response of the detectors to varying amount of toluene was achieved using gravimetrically prepared mixtures of toluene-heptane (where toluene is diluted) with different compositions. The densities of the pure toluene and pure heptane used to prepare the calibration mixtures were obtained using reference equations developed by Lemmon and Span [35] and Span and Wagner [36], respectively, which have estimated relative uncertainties of 0.05% and 0.2% respectively. The densities of the resulting mixtures were estimated using the GERG-2008 EOS [14], with an estimated relative uncertainties of 0.2% for the mixture density.

A linear relationship between the amount of toluene present and the FID or BID response area was observed. This is mainly because in both cases a sufficiently small amount of toluene was present. Therefore, a linear equation was used to fit the response area as a function of toluene amount. However, a nonlinear relationship between the amount of methane or propane present and the FID or BID response area was observed at conditions because a much wider range of sample concentration was considered for these compounds. Accordingly, a quadratic polynomial was used to fit the response area relative to the amounts of each component injected. Examples showing the response area of the FID detector are presented in Figure 3, for methane and propane, where hydrogen was used as a carrier gas.



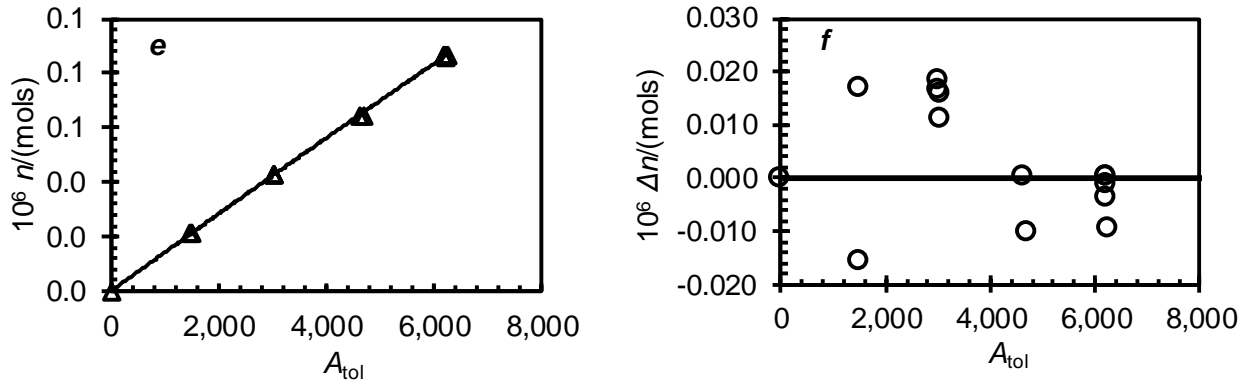


Figure 3. Flame Ionization Detector (FID) calibration data for methane (a and b), propane (c and d) and toluene (e and f): (a), (c) and (e), number of moles, n , at the filling-loop conditions against area response A ; (b), (d) and (f), deviations, Δn , of the number of moles injected from the value predicted with the polynomial equation fitted against area response A .

The standard relative uncertainty in the peak area during calibration was typically around 1% for each component but for some cases, especially for toluene, the deviation went up to few percent. This deviation was considered in the uncertainty calculations. The GC calibrations for methane and propane were validated with a gravimetrically prepared mixture of (0.8180CH₄ + 0.1820C₃H₈).

The uncertainties of the mole fractions of each component, $u(y_i)$, in the gravimetrically prepared gas mixture, were calculated from:

$$u(y_i) = \left(\frac{1}{\sum_{j=1}^N n_j} \right) \sqrt{(1-2y_i)u(n_i)^2 + y_i^2 \sum_{j=1}^N u(n_j)^2}, \quad (1)$$

Here n is the number of moles of a component added to the mixture, calculated from the mass of the gas added. The standard uncertainty in the mole fraction $u(x)$ of the gravimetrically prepared mixture was estimated to be 0.0005.

The measured mole fraction from the GC analysis was found as (0.8144CH₄ + 0.1856C₃H₈). The measured mole fraction is less than 0.4% deviation from the mole fraction of the gravimetrically prepared mixture, which is within the overall uncertainty in the measured mole fraction.

2.5 Uncertainty Analysis

Contributions to the combined standard uncertainty in the measured mole fractions, z_i , were considered with reference to equation (10) presented in the “Guide to the Expression of Uncertainty in Measurement” [37] (commonly known as GUM):

$$u^2(x_i) = \sum_{j=1}^n \left[\left(\frac{\partial x_i}{\partial z_j} \right)^2 u^2(z_j) \right] \quad (2)$$

where z_j ($j = 1, 2, 3 \dots n$) are the n independent variables upon which x_i is dependent, each associated with variance $u^2(z_j)$.

A detailed description of the uncertainty analysis can be found in our previous work [20, 30, 31]. Overall, the uncertainty in the mole fraction obtained in both apparatus is calculated from the following equation:

$$u^2(x_i) = (\partial x_i / \partial T)^2 u^2(T) + (\partial x_i / \partial p)^2 u^2(p) + \sum_{j \neq i} (x_i x_j)^2 [u_r^2(f_j) + u_r^2(A_j)] + [x_i(1 - x_i)]^2 [u_r^2(f_i) + u_r^2(A_i)], \quad (3)$$

where $u_r(X)$ denotes the standard relative uncertainty of variable X , f_i is the chromatographic response factor and A_i is the chromatographic peak area. The variables that mainly contribute to the overall uncertainties in the mole fraction measurements are uncertainties associated with the calibration and area relationships from the GC measurements. In addition to the GC calibration factors, the effect of the temperature and pressure uncertainty on the composition measurements were also considered as contributors to the combined uncertainty.

The uncertainty of the mole fraction arising from the peak area and GC calibration were determined by the standard deviation of the peak area during sampling, the uncertainties during calibration of both the peak area and the calculated amount of substance for that pure component, the latter being affected by the uncertainties of pressure, temperature, calibration method used, and the equation of state from which the density is calculated. The uncertainties due to pressure and temperature on the resulting phase compositions were calculated from the standard uncertainty of the temperature and pressures as well as the partial derivatives of the mole fractions with respect to temperature and pressure. This leads to overall combined standard uncertainties of mole fraction that vary over a wide range depending upon the component, temperature, pressure, and phase in question, as presented in Tables 2 and 3.

3. Results and Model Comparison

Measurements were completed along isochoric pathways with each apparatus: isochores 1, 2 and 3 were measured with the Cryostat VLE cell at temperatures between 213 K and 273 K. Isochores A, B, C and D were measured with the Bath VLE cell at temperatures range between 257 K and 298 K. In Tables 2 and 3 a total of 38 new dew point and 38 new bubble point VLE data for (methane + propane + toluene) ternary system are presented. The focus of the Cryostat VLE cell in particular was to investigate systems with very low toluene fractions. The *maximum* liquid mole fraction of toluene in those experiments was 0.0379. For the Bath VLE cell, a wider range of toluene fractions was studied with the *minimum* liquid mole fraction of toluene being 0.160.

The predictions of the PR EOS implemented in HYSYS, which is frequently used throughout the oil and gas industry, particularly when simulating industrial LNG scrub columns, were tested against the new VLE data. Figure 4 shows the measurement p - T conditions of the data measured for Isochores 1, 2 and 3. Figure 4 also shows a VLE phase envelope (green) calculated using the HYSYS PR EOS for the saturated vapor phase measured at $T = 273.09$ K and $p = 6.515$ MPa.

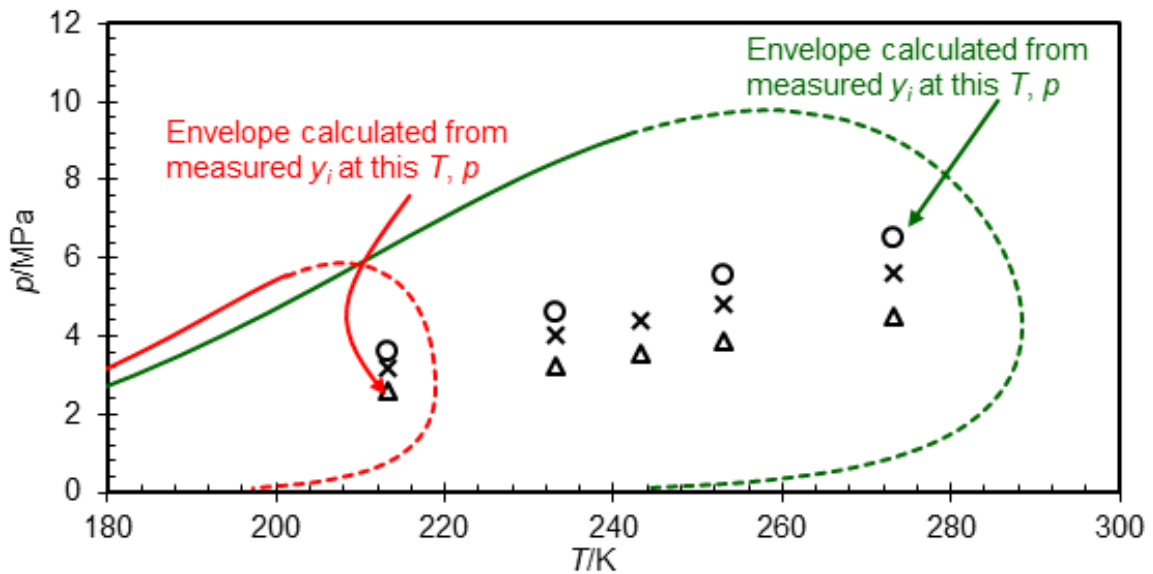


Figure 4. Pressure-temperature conditions of VLE measurements completed with the Cryostat VLE cell: O, isochore 1; X, isochore 2; Δ, isochore 3.

The predicted upper dew pressure for this (0.844 CH₄ + 0.155 C₃H₈ + 0.00127 C₇H₈) mixture at $T = 273.09$ K is 9.039 MPa. This is about 2.5 MPa or 39 % higher than the measured upper dew pressure. The substantial over-prediction by the EOS of the upper dew pressure occurs because the specified (measured) vapor composition contains a much higher toluene content than what the EOS would predict at that (p, T) condition. Figure 4 also shows a second phase envelope (red) calculated using the HYSYS PR EOS for the leanest saturated vapor phase measured at $T = 213.16$ K and $p = 2.601$ MPa. The predicted upper dew point of this (0.9756 CH₄ + 0.0244 C₃H₈ + 0.0000130 C₇H₈) mixture at $T = 213.16$ K is 5.565 MPa, about 3.0 MPa or 114 % higher than the measured upper dew pressure. These results demonstrate that the amount of toluene carried in the vapor phase is substantially higher than predicted by the standard HYSYS PR EOS, which is of significant concern for assessments of the amount of toluene (or other BTEX aromatics) carried over to the MCHE.

Figure 5 shows the measurement p - T conditions of the data measured for Isochores A, B, C and D. The phase envelope (green) was calculated using HYSYS PR EOS for the saturated vapor phase measured at $T = 298.10$ K and $p = 9.842$ MPa. The predicted upper dew pressure for this (0.8246 CH₄ + 0.1701 C₃H₈ + 0.00526 C₇H₈) mixture is 10.25 MPa, about 0.4 MPa or 4.1 % higher than the measured pressure. A second phase envelope (red) is also shown, calculated for a leaner saturated vapor phase at $T = 257.70$ K and $p = 6.265$ MPa. The calculated upper dew pressure for this (0.9278 CH₄ + 0.0717 C₃H₈ + 0.000507 C₇H₈) mixture is 6.798 MPa, about 0.5 MPa or 8.5 % higher than the measured pressure. While the errors in the predicted dew pressures are smaller than those observed at lower temperatures for leaner toluene contents, these results also demonstrate that substantially more toluene can be solvated into the vapor phase than predicted by the industry-standard HYSYS PR EOS.

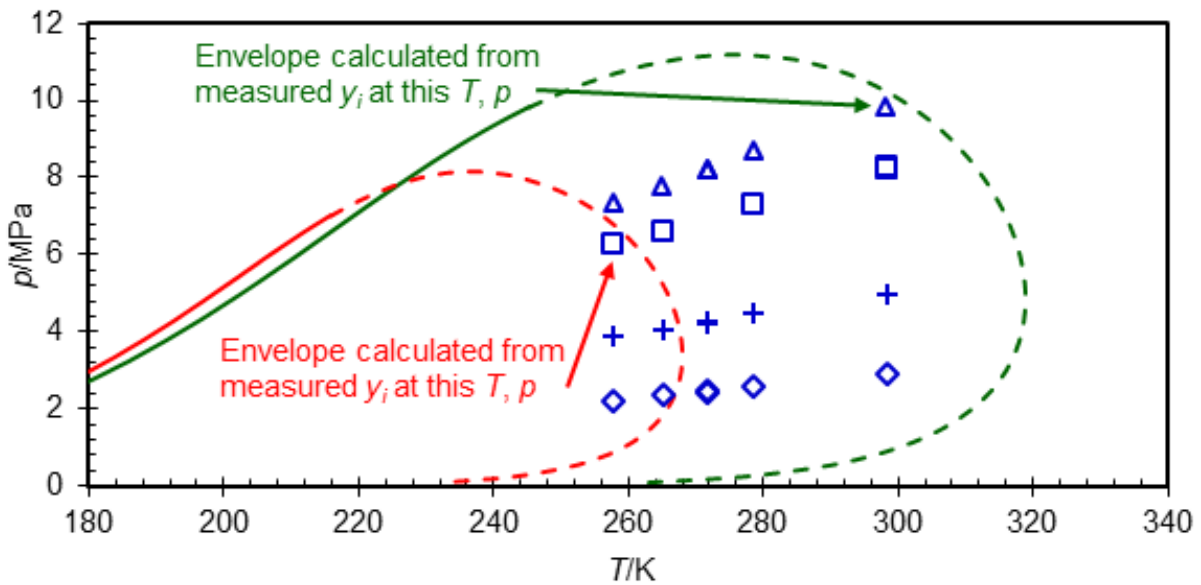


Figure 5. Pressure-temperature conditions of VLE measurements completed with the bath VLE cell: \square , isochore A; $+$, isochore B, \diamond , isochore C; \triangle , isochore D

Table 2. Dew Temperatures, Pressures and Mole Fractions for Methane (1) + Propane (2) + Toluene (3) mixtures.

T_{dew}/K	$u(T_{\text{dew}})/K$	p/MPa	$u(p)/\text{MPa}$	y_1	y_2	y_3	$u(y_1)$	$u(y_2)$	$u(y_3)$
Isochore 1									
213.15	0.17	3.608	0.002	0.9679	0.0321	*	0.00159	0.00152	*
233.11	0.15	4.611	0.002	0.9493	0.0498	0.00094	0.00229	0.00226	0.000111
253.10	0.16	5.584	0.003	0.9079	0.0908	0.00134	0.00392	0.00390	0.000157
273.09	0.14	6.515	0.002	0.844	0.155	0.00127	0.00618	0.00616	0.000148
Isochore 2									
273.10	0.16	5.601	0.003	0.8447	0.1549	0.000381	0.00616	0.00616	0.000045
213.14	0.17	3.174	0.010	0.9684	0.0316	*	0.00151	0.00151	*
233.12	0.20	4.005	0.002	0.9512	0.0487	0.000106	0.00222	0.00222	0.000013
253.10	0.16	4.808	0.002	0.9078	0.0918	0.00043	0.00394	0.00394	0.000050
243.10	0.16	4.395	0.050	0.9323	0.0674	0.000238	0.00299	0.00298	0.000028
Isochore 3									
273.10	0.16	4.485	0.002	0.8350	0.1647	0.000339	0.00647	0.00647	0.000040
233.13	0.18	3.247	0.002	0.9473	0.0527	0.0000541	0.00239	0.00238	0.000006
243.12	0.19	3.563	0.002	0.9266	0.0732	0.000126	0.00322	0.00322	0.000015
253.11	0.18	3.855	0.003	0.9017	0.0982	0.0001501	0.00418	0.00418	0.000018
213.16	0.20	2.601	0.002	0.9756	0.0244	0.0000130	0.00121	0.00121	0.000002
Isochore A									
298.30	0.20	8.218	0.001	0.8582	0.1380	0.003808	0.0030	0.0030	0.000089
257.70	0.20	6.265	0.001	0.9278	0.0717	0.000507	0.0017	0.0017	0.000020
265.06	0.20	6.616	0.001	0.9147	0.0846	0.000777	0.0020	0.0020	0.000024
278.69	0.20	7.285	0.001	0.8899	0.1085	0.001598	0.0025	0.0024	0.000041
298.32	0.20	8.269	0.001	0.8573	0.1389	0.003870	0.0030	0.0030	0.000090
Isochore B									
298.29	0.20	4.946	0.001	0.8402	0.1574	0.002383	0.0033	0.0033	0.000057
271.79	0.20	4.218	0.001	0.8933	0.1061	0.000635	0.0024	0.0024	0.000022

T_{dew}/K	$u(T_{\text{dew}})/K$	p/MPa	$u(p)/\text{MPa}$	y_1	y_2	y_3	$u(y_1)$	$u(y_2)$	$u(y_3)$
271.79	0.20	4.220	0.001	0.9027	0.0967	0.000631	0.0022	0.0022	0.000022
257.79	0.20	3.871	0.001	0.9214	0.0783	0.000277	0.0019	0.0019	0.000017
265.09	0.20	4.070	0.001	0.9073	0.0922	0.000426	0.0021	0.0021	0.000019
271.82	0.20	4.266	0.001	0.8936	0.1058	0.000640	0.0024	0.0024	0.000022
278.65	0.20	4.464	0.001	0.8798	0.1193	0.000934	0.0027	0.0026	0.000027
Isochore C									
271.80	0.20	2.438	0.001	0.8614	0.1380	0.000638	0.0030	0.0030	0.000022
257.76	0.20	2.223	0.001	0.8962	0.1036	0.000279	0.0024	0.0023	0.000017
265.10	0.20	2.343	0.001	0.8785	0.1210	0.000425	0.0027	0.0027	0.000019
271.79	0.20	2.460	0.001	0.8622	0.1372	0.000638	0.0030	0.0030	0.000022
278.63	0.20	2.581	0.001	0.8454	0.1536	0.000934	0.0032	0.0032	0.000027
298.27	0.20	2.921	0.001	0.8004	0.1971	0.002475	0.0039	0.0039	0.000058
Isochore D									
257.66	0.20	7.347	0.001	0.9193	0.0799	0.000742	0.0019	0.0019	0.000024
264.95	0.20	7.789	0.001	0.9041	0.0948	0.001083	0.0022	0.0022	0.000030
271.64	0.20	8.231	0.001	0.8904	0.1081	0.001530	0.0024	0.0024	0.000039
271.64	0.20	8.231	0.001	0.8891	0.1093	0.001595	0.0025	0.0025	0.000040
278.48	0.20	8.703	0.001	0.8737	0.1239	0.002311	0.0027	0.0027	0.000056
298.10	0.20	9.842	0.001	0.8246	0.1701	0.005261	0.0035	0.0035	0.000120

* vapor phase toluene gas chromatogram peaks below signal to noise ratio and not possible to quantify.

Table 3. Bubble Temperatures, Pressures and Mole Fractions for Methane (1) + Propane (2) + Toluene (3) mixtures.

T_{bub}/K	$u(T_{\text{bub}})/K$	p/MPa	$u(P)/\text{MPa}$	x_1	x_2	x_3	$u(x_1)$	$u(x_2)$	$u(x_3)$
Isochore 1									
213.14	0.17	0.998	0.001	0.467	0.508	0.02518	0.0115	0.0116	0.0028
233.11	0.15	4.604	0.001	0.439	0.535	0.0258	0.0114	0.0115	0.0029
253.10	0.16	5.575	0.002	0.417	0.556	0.0277	0.0113	0.0114	0.0031
273.09	0.14	6.525	0.003	0.400	0.570	0.0299	0.0111	0.0113	0.0034
Isochore 2									
273.10	0.16	5.612	0.002	0.3379	0.6276	0.0344	0.0104	0.0108	0.0039
213.14	0.17	3.179	0.001	0.4061	0.5639	0.02995	0.0112	0.0113	0.0034
233.11	0.16	4.000	0.001	0.3788	0.5915	0.02964	0.0109	0.0111	0.0033
253.10	0.16	4.793	0.003	0.3556	0.6131	0.03122	0.0106	0.0109	0.0035
243.10	0.16	4.412	0.001	0.3666	0.6030	0.03038	0.0108	0.0110	0.0034
Isochore 3									
273.10	0.16	4.507	0.001	0.2624	0.6997	0.0379	0.0090	0.0098	0.0042
233.13	0.18	3.255	0.001	0.3291	0.6388	0.0321	0.0102	0.0106	0.0036
243.12	0.19	3.547	0.003	0.2935	0.6719	0.03457	0.0096	0.0102	0.0039
253.11	0.18	3.873	0.001	0.2908	0.6745	0.03471	0.0096	0.0102	0.0039
213.16	0.20	2.600	0.003	0.329	0.636	0.035	0.0102	0.0107	0.0039
Isochore A									
298.29	0.20	8.218	0.001	0.2654	0.3743	0.3603	0.0041	0.0050	0.0050
257.71	0.20	6.265	0.001	0.3230	0.4327	0.2444	0.0047	0.0053	0.0040
265.06	0.20	6.616	0.001	0.3133	0.4317	0.2550	0.0046	0.0053	0.0041
278.69	0.20	7.285	0.001	0.2907	0.4150	0.2944	0.0044	0.0052	0.0045
298.31	0.20	8.281	0.001	0.2676	0.3723	0.3602	0.0042	0.0050	0.0050

T_{bub}/K	$u(T_{\text{bub}})/K$	p/MPa	$u(P)/\text{MPa}$	x_1	x_2	x_3	$u(x_1)$	$u(x_2)$	$u(x_3)$
Isochore B									
298.29	0.20	4.945	0.001	0.1497	0.3846	0.4657	0.0027	0.0053	0.0055
271.79	0.20	4.218	0.001	0.1708	0.4526	0.3766	0.0030	0.0054	0.0052
271.81	0.20	4.222	0.001	0.1724	0.4594	0.3682	0.0030	0.0054	0.0052
257.80	0.20	3.870	0.001	0.1878	0.4745	0.3376	0.0033	0.0054	0.0049
265.10	0.20	4.070	0.001	0.1791	0.4646	0.3563	0.0031	0.0054	0.0051
271.82	0.20	4.267	0.001	0.1734	0.4499	0.3767	0.0030	0.0054	0.0052
278.66	0.20	4.464	0.001	0.1689	0.4356	0.3955	0.0030	0.0054	0.0053
Isochore C									
271.79	0.20	2.437	0.001	0.0895	0.4225	0.4880	0.0017	0.0056	0.0057
257.78	0.20	2.223	0.001	0.0962	0.4530	0.4508	0.0018	0.0056	0.0057
265.11	0.20	2.341	0.001	0.0915	0.4384	0.4701	0.0018	0.0056	0.0057
271.81	0.20	2.455	0.001	0.0898	0.4217	0.4885	0.0017	0.0056	0.0057
278.62	0.20	2.580	0.001	0.0862	0.4065	0.5074	0.0017	0.0056	0.0057
298.26	0.20	2.930	0.001	0.0814	0.3488	0.5697	0.0016	0.0053	0.0056
Isochore D									
257.67	0.20	7.358	0.001	0.4045	0.4357	0.1598	0.0053	0.0054	0.0029
264.97	0.20	7.813	0.001	0.3975	0.4330	0.1695	0.0052	0.0054	0.0031
271.64	0.20	8.231	0.001	0.3862	0.4331	0.1807	0.0052	0.0054	0.0032
271.64	0.20	8.231	0.001	0.3892	0.4315	0.1793	0.0052	0.0054	0.0032
278.52	0.20	8.745	0.001	0.3810	0.4250	0.1940	0.0051	0.0053	0.0034
298.14	0.20	9.830	0.001	0.3421	0.3980	0.2599	0.0048	0.0051	0.0041

An alternative means of interpreting the measured data is to consider the dew point temperatures calculated using the HYSYS PR EOS from the measured pressures and vapor mole fractions. Two examples of such analyses are shown in Figure 6 for isochores 3 (a & b) and A (c & d), respectively. Shown in part (a & c) of these figures is the measured temperature as a function of the measured toluene mole fraction in the vapor phase. In part (b & d) a deviation plot of the difference between the measured and HYSYS PR EOS calculated dew temperature is shown.

In both of these plots, the difference is always negative, which indicates that the true dew temperature is significantly lower than calculated by the HYSYS PR EOS. For a specified vapor composition, an over prediction of the dew point temperature means the EOS *under* predicts the amount of toluene that can be present in the saturated vapor. For isochore 3 the measured dew temperature was between 5.6 and 2.6 K lower than that predicted. For isochore A, the measured dew temperature was between 3.2 and 3.8 K lower than that calculated using the HYSYS PR EOS.

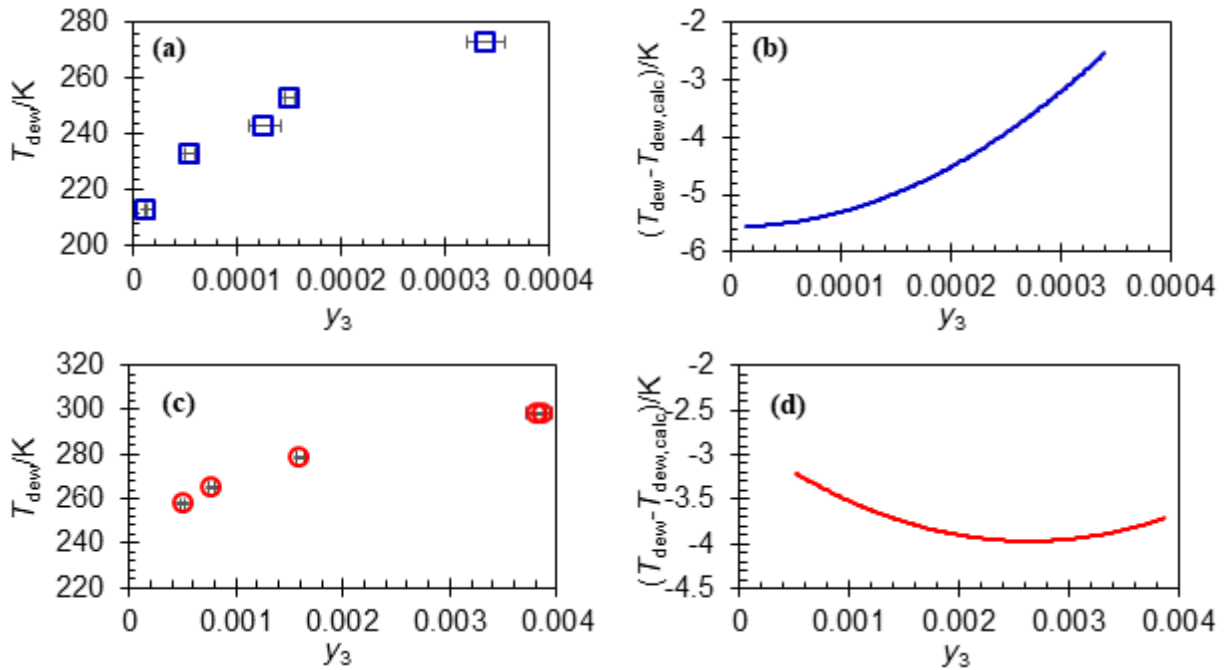


Figure 6. (a) Dew temperature, T_{dew} , as a function of mole fraction of toluene in the vapor phase, y_3 , for isochore 3. (b) Deviation between the measured dew temperature and that calculated by the HYSYS PR EOS, $T_{\text{dew,calc}}$. (c) Dew temperature, T_{dew} , as a function of mole fraction of toluene in the vapor phase, y_3 , for isochore A. (d) Deviation between the measured dew temperature and that calculated by the HYSYS PR EOS, $T_{\text{dew,calc}}$.

Clearly these VLE measurements unambiguously demonstrate that the HYSYS PR EOS substantially under-predicts the possible toluene content of saturated vapors that could be present in the overhead of the LNG scrub column. The error in the prediction increases with decreasing temperature: for isochores 1-3, (average temperature near 240 K), the average relative error in the predicted vapor phase content was 77 %, while for isochores A-D, the average relative error was 12.7 %. This result also underscores the importance of improving predictions of the allowable threshold concentration of BTEX in fluids entering the MCHE to avoid potential freeze-out.

A small upset in the carry-over of heavy hydrocarbons can lead to build-up of BTEX inside the MCHE sufficient to eventually cause blockage issues and thus a plant shutdown if no remedial action is taken. To illustrate the significance of accurately predicting the concentration of aromatics in the vapour overheads entering the MCHE, solid-liquid equilibrium temperatures at $p = 5$ MPa were evaluated for the ternary mixture $[0.9323 C_1 + 0.0674 C_3 + 0.000238 C_7]$ measured along Isochore 2. This was then evaluated using the ThermoFAST model recently developed and optimised for SLE calculations [13, 38] which has been tuned to all literature experimental data including the SLE data measured in our laboratories [39-41]. Effluent LNG leaving the MCHE is normally at a condition around (120 K, 3.5 MPa) [13], so to avoid any risk of blockage, the SLE temperature for any mixture entering the heat exchanger should be significantly lower than 120 K at this pressure. The SLE temperature at 3.5 MPa of the $[0.9323 C_1 + 0.0674 C_3 + 0.000238 C_7]$ mixture measured in this work is estimated using ThermoFAST to be 120.3 K, which is of sufficient concern that plant operators or engineers might take remedial action. However, such a

concentration of toluene is not readily measurable using plant GCs, which typically can only resolve BTEX separately from other C₆₊ compounds. Thus operators and engineers rely on *predictions* of saturated vapour composition, and the results of this work indicate that such predictions will underestimate the toluene content by 77 % on average. The SLE temperature at 3.5 MPa predicted by ThermoFAST for a ternary mixture with 77 % lower toluene concentration is 113.7 K. This might lead to the conclusion that the blockage risk is minimal when in fact it might be appreciable.

4. Conclusion

New VLE data for the ternary mixture [methane + propane + toluene] have been measured at conditions relevant to the operation of LNG scrub columns. The mixture was studied over a wide range of conditions with toluene as the minor component in both the liquid and vapor phases. Measurements were conducted along different isochoric paths at temperatures between (213 and 298 K) and pressures up to 8.3 MPa. These data provide an opportunity to test the performance of the equations of state used widely in the design and operation of different processes in the natural gas and LNG industry.

The measured VLE data were compared here to results calculated with the HYSYS Peng Robinson (PR) equation of state (EOS) that is used widely in LNG industry. The amount of toluene in the vapour phase was found to be under-predicted by the HYSYS PR EOS by an average of around 77 % at lower temperatures, with the error increasing as temperature and toluene concentration decreased. These VLE measurements unambiguously demonstrate that the PR EOS as well as other cubic EOS implemented in most process simulators substantially under-predict the possible toluene content of saturated vapours that could be present in the overhead of the LNG scrub column. The current work also underscores the importance of improving predictions of the allowable threshold concentration of heavy components in fluids entering the MCHE so as to avoid potential freeze-out. An under-prediction of the toluene concentration in a saturated vapour by 77 % could risk the under-prediction of solid-liquid equilibrium temperatures by 7 K. Such a difference could constitute the difference between a negligible and appreciable risk of blocking the MCHE in an LNG plant.

5. Acknowledgements

This work was funded by the ARC Training Centre for LNG Futures (Australian Research Council grant number IC150100019). We thank Stanley Huang and Jeff Buckles of Chevron for helpful discussions.

6. References

[1] A.J.P. Kidnay, W, Fundamentals of Natural Gas Processing, CRC Press (2011).

- [2] M. Baccanelli, S. Langé, M.V. Rocco, L.A. Pellegrini, E. Colombo, Low temperature techniques for natural gas purification and LNG production: An energy and exergy analysis, *Appl. Energy*, 180 (2016) 546-559.
- [3] A. Madouri, Improvement of high heating value of commercialised liquefied natural gas of GL1Z plant by optimising the LPG extraction, LNG-14, Doha, Qatar, (2004).
- [4] K. Kaneko, K. Ohtani, Y. Tsujikawa, S. Fujii, Utilization of the cryogenic exergy of LNG by a mirror gas-turbine, *Appl. Energy*, 79 (2004) 355-369.
- [5] M. Baccanelli, S. Langé, M.V. Rocco, L.A. Pellegrini, E. Colombo, Low temperature techniques for natural gas purification and LNG production: An energy and exergy analysis, *Appl. Energy*, 180 (2016) 546-559.
- [6] W. Lim, K. Choi, I. Moon, Current status and perspectives of Liquefied Natural Gas (LNG) plant design, *Ind. Eng. Chem. Res.*, 52 (2013) 3065-3088.
- [7] H.M. Chang, A thermodynamic review of cryogenic refrigeration cycles for liquefaction of natural gas, *Cryogenics*, 72 (2015) 127-147.
- [8] M.S. Khan, S. Lee, G.P. Rangaiah, M. Lee, Knowledge based decision making method for the selection of mixed refrigerant systems for energy efficient LNG processes, *Appl. Energy*, 111 (2013) 1018-1031.
- [9] A. Mortazavi, C. Somers, Y. Hwang, R. Radermacher, P. Rodgers, S. Al-Hashimi, Performance enhancement of propane pre-cooled mixed refrigerant LNG plant, *Appl. Energy*, 93 (2012) 125-131.
- [10] F. Dauber, R. Span, Modelling liquefied-natural-gas processes using highly accurate property models, *Appl. Energy*, 97 (2012) 822-827.
- [11] F. Dauber, R. Span, Achieving higher accuracies for process simulations by implementing the new reference equation for natural gases, *Comput. Chem. Eng.*, 37 (2012) 15-21.
- [12] M. Thol, E.W. Lemmon, R. Span, Equation of state for benzene for temperatures from the melting line up to 725 K with pressures up to 500 MPa, *High Temperatures -- High Pressures*, 41 (2012) 81-97.
- [13] C.J. Baker, J.H. Oakley, D. Rowland, T.J. Hughes, Z.M. Aman, E.F. May, Rapid Simulation of Solid Deposition in Cryogenic Heat Exchangers To Improve Risk Management in Liquefied Natural Gas Production, *Energy Fuels*, 32 (2018) 255-267.
- [14] O. Kunz, W. Wagner, The GERG-2008 Wide-Range Equation of State for Natural Gases and Other Mixtures: An Expansion of GERG-2004, *J. Chem. Eng. Data*, 57 (2012) 3032-3091.
- [15] R.A. Russel, A Flexible and Reliable Method Solves Single-Tower and Crude-Distillation-Column Problems, *Chem. Eng.*, 90 (1983) 53-59.
- [16] C.L. Rhodes, The Process Simulation Revolution: Thermophysical Property Needs and Concerns, *J. Chem. Eng. Data*, 41 (1996) 947-950.
- [17] J.C. Rainwater, D.G. Friend, H.J.M. Hanley, A.H. Harvey, C.D. Holcomb, A. Laesecke, J.W. Magee, C. Muzny, Forum 2000: Fluid Properties for New Technologies, Connecting Virtual Design with Physical Reality, *J. Chem. Eng. Data*, 46 (2001) 1002-1006.

- [18] H.Z. Kister, Can We Believe the Simulation Results, Chem. Eng. Prog., 98 (2002) 52-58.
- [19] E.F. May, A. Vieler, T.J. Hughes, Y. Wicaksana, G. Byfield, D. Hodges, Benchmarking LNG Process Simulation Against Operational Plant Data, Proceedings of LNG-18, Perth Australia, (2016).
- [20] E.F. May, J.Y. Guo, J.H. Oakley, T.J. Hughes, B.F. Graham, K.N. Marsh, S.H. Huang, Reference Quality Vapor–Liquid Equilibrium Data for the Binary Systems Methane + Ethane, + Propane, + Butane, and + 2-Methylpropane, at Temperatures from (203 to 273) K and Pressures to 9 MPa, J. Chem. Eng. Data, 60 (2015) 3606-3620.
- [21] D. Rowland, T.J. Hughes, E.F. May, Extending the GERG-2008 Equation of State: Improved Departure Function and Interaction Parameters for (Methane + Butane), J. Chem. Thermodyn., doi: <http://dx.doi.org/10.1016/j.jct.2016.01.005> (2016).
- [22] D.-Y. Peng, D.B. Robinson, A New Two-Constant Equation of State, Ind. Eng. Chem. Fundam., 15 (1976) 59-64.
- [23] G. Soave, Equilibrium Constants from a Modified Redlich-Kwong Equation of State, Chem. Eng. Sci., 27 (1972) 1197-1203.
- [24] T.J. Hughes, M.E. Kandil, B.F. Graham, K.N. Marsh, S.H. Huang, E.F. May, Phase Equilibrium Measurements of (Methane + Benzene) and (Methane + Methylbenzene) at Temperatures from (188 to 348) K and Pressures to 13 MPa, J. Chem. Thermodyn., 85 (2015) 141-147.
- [25] M.E. Kandil, M.J. Thoma, T. Syed, J. Guo, B.F. Graham, K.N. Marsh, S.H. Huang, E.F. May, Vapor-Liquid Equilibria Measurements of the Methane + Pentane and Methane + Hexane Systems at Temperatures from (173 to 330) K and Pressures to 14 MPa, J. Chem. Eng. Data, 56 (2011) 4301-4309.
- [26] AspenTech, Aspen HYSYS Process Simulator, v8.6, Aspen Technology, Inc, Cambridge, MA, 2016.
- [27] T.J. Hughes, M.E. Kandil, B.F. Graham, E.F. May, Simulating the Capture of CO₂ from Natural Gas: New Data and Improved Models for Methane + Carbon Dioxide + Methanol, Int. J. Greenhouse Gas Control, 31 (2014) 121-127.
- [28] M.E. Kandil, E.F. May, B.F. Graham, K.N. Marsh, M.A. Trebble, R.D. Trengove, S.H. Huang, Vapor-Liquid Equilibria Measurements of Methane + 2-Methylpropane (Isobutane) at Temperatures from (150 to 250) K and Pressures to 9 MPa, J. Chem. Eng. Data, 55 (2010) 2725-2731.
- [29] E.F. May, M. S, M.E. Kandil, B.F. Graham, K.N. Marsh, S.H. Huang, Measurement and Modeling of VLE in Binary Systems of CH₄ + {C₅, C₆, or BTX Compounds} at Cryogenic Temperatures and High Pressures, in: 90th Annual Convention of the Gas Processors Association, San Antonio TX, 2011.
- [30] S.Z. Al Ghafri, E. Forte, G.C. Maitland, J.J. Rodriguez-Henríguez, J.M. Trusler, Experimental and modeling study of the phase behavior of (methane+ CO₂+ water) mixtures, J. Phys. Chem. B, 118 (2014) 14461-14478.

- [31] S.Z. Al Ghafri, E. Forte, A. Galindo, G.C. Maitland, J.M. Trusler, Experimental and Modeling Study of the Phase Behavior of (Heptane+ Carbon Dioxide+ Water) Mixtures, *J. Chem. Eng. Data*, 60 (2015) 3670-3681.
- [32] S.Z.S. Al Ghafri, J.P.M. Trusler, Phase equilibria of (Methylbenzene + Carbon dioxide + Methane) at elevated pressure: Experiment and modelling, *J. Supercrit. Fluids*, 145 (2019) 1-9.
- [33] U. Setzmann, W. Wagner, A New Equation of State and Tables of Thermodynamic Properties for Methane Covering the Range from the Melting Line to 625 K at Pressures up to 1000 MPa, *J. Phys. Chem. Ref. Data*, 20 (1991) 1061-1151.
- [34] E.W. Lemmon, M.O. McLinden, W. Wagner, Thermodynamic Properties of Propane. III. A Reference Equation of State for Temperatures from the Melting Line to 650 K and Pressures up to 1000 MPa, *J. Chem. Eng. Data*, 54 (2009) 3141-3180.
- [35] E.W. Lemmon, R. Span, Short Fundamental Equations of State for 20 Industrial Fluids, *J. Chem. Eng. Data*, 51 (2006) 785-850.
- [36] R. Span, W. Wagner, Equations of State for Technical Applications. II. Results for Nonpolar Fluids, *Int. J. Thermophys.*, 24 (2003) 41-109.
- [37] Joint Committee for Guides in Metrology, Evaluation of Measurement Data - Guide to the Expression of Uncertainty in Measurement (GUM:1995 with Minor Corrections), in, Bureau International des Poids et Mesure, Sèvres, France, 2008.
- [38] C. Baker, A. Siahvashi, J. Oakley, T. Hughes, D. Rowland, S. Huang, E.F. May, Advanced predictions of solidification in cryogenic natural gas and LNG processing, *J. Chem. Thermodyn.*, 137 (2019) 22-33.
- [39] A. Siahvashi, S.Z.S. Al-Ghafri, J.H. Oakley, T.J. Hughes, B.F. Graham, E.F. May, Visual Measurements of Solid Liquid Equilibria and Induction Times for Cyclohexane + Octadecane Mixtures at Pressures to 5 MPa, *J. Chem. Eng. Data*, 62 (2017) 2896-2910.
- [40] A. Siahvashi, S.Z. Al Ghafri, T.J. Hughes, B.F. Graham, S.H. Huang, E.F. May, Solubility of p-xylene in methane and ethane and implications for freeze-out at LNG conditions, *Exp. Therm. Fluid Sci.*, 105 (2019) 47-57.
- [41] A. Siahvashi, Visual Measurements of Solid-Fluid Equilibria in Hydrocarbon Mixtures for Enhanced LNG Production, in: Chemical Engineering Department, PhD Thesis, The University of Western Australia, 2019.